Mathematical Biosciences and Engineering

MBE, 19 (5), 4643–4656.
DOI: 10.3934/mbe.2022215
Received: 30 September 2021
Revised: 04 December 2021
Accepted: 19 January 2022
Published: 07 March 2022

http://www.aimspress.com/journal/MBE

Research article

Unified implementation of global high dynamic range image tone-mapping algorithms

Ishtiaq Rasool Khan[1,*] and Susanto Rahardja[2]

[1] Department of Computer Science and Artificial Intelligence, College of Computer Science and Engineering, University of Jeddah, Jeddah 21589, Saudi Arabia
[2] School of Marine Science and Technology, Northwestern Polytechnical University, 127 West Youyi Road, Xi'an, Shaanxi 710072, China

* **Correspondence:** Email: irkhan@uj.edu.sa.

Abstract: High dynamic range (HDR) images and video require tone-mapping for display on low dynamic range (LDR) screens. Many tone-mapping operators have been proposed to convert HDR content to LDR, but almost each has a different implementation structure and requires a different execution time. We propose a unified structure that can represent any global tone-mapping algorithm with an array of just 256 coefficients. These coefficients extracted offline for every HDR image or video frame can be used to convert them to LDR in real time using linear interpolation. The produced LDR images are identical to the images produced by the original implementation of the algorithm. This unified implementation can replicate any global tone-mapping function and requires very low and fixed execution time, which is independent of algorithm and type of content and depends only on image size. Experimental studies are presented to show the accuracy and time efficiency of the proposed implementation.

Keywords: high dynamic range imaging; tone-mapping; unified implementation of TMO; HDR display; generic TMO design

1. Introduction

HDR images capture a larger range of luminance than their LDR counterparts, which leads to improved visual quality and user experience. Moreover, HDR images can be helpful in applications

like image-based scene analysis. Recent advances in hardware and software technologies have made it possible to capture high-quality HDR images and video. However, despite a rapid increase in market share, HDR displays are unlikely to replace or outnumber the existing LDR displays soon. Therefore, the development of algorithms to transform HDR images to LDR, known as tone-mapping operators (TMOs), remains an active research area.

TMOs leverage rich HDR content and generally use the human visual system (HVS) characteristics to produce visually pleasing LDR images. TMOs can be classified into two major categories—global, which maps a pixel solely based on its luminance value, and local, which also takes pixel intensities in the neighborhood into account. Local tone-mapping algorithms, in general, are good at preserving details by utilizing the local features in each region; however, they may induce halo and other artifacts [1]. In some subjective studies [2], the participants predominantly preferred global TMOs over the local algorithms due to the naturalness of the output images.

The transformation curves used for tone-mapping are content-dependent, in general, which means that a new mapping needs to be designed for each image. In addition, most of the TMOs have complex operations and are not suitable for real time processing. Tone-mapping operation can be thought as a two-step process, designing the mapping function, and applying it to the HDR image. Some TMOs that use a global transformation or linear interpolation can be applied efficiently [3–5], but designing these transformations for each image is still computationally heavy. Therefore the common industry practice is to produce duplicate LDR and HDR versions of the same content to cater to the needs of both display types, which can be laborious and expensive in terms of bandwidth and storage [6]. From the production perspective, it is desirable to keep the contents in HDR format only and compress their dynamic range through tone-mapping [1] when the target display is LDR.

In this paper, we show that it is possible to represent the design of any global TMO accurately using an array of 256 floating-point values. This array can be used to tone-map the HDR image very efficiently through linear interpolation. We propose to pre-construct the array offline and store it with the HDR image and perform the interpolation in real time for display. The tone-mapped image is generated first by the original algorithm at the offline stage and 256 coefficients are extracted from the pair of the HDR image and its tone-mapped version. We present a simple method to extract these coefficients. The output of the original TMO and that generated by using the proposed technique remain identical. In a study by Cerdá-Company et al. [2], TMOs proposed by Kim et al. [7] and Reinhard et al. [5] were observed to produce significantly better results than other evaluated algorithms. We present design examples converting these two TMOs to our proposed unified 256×1 format.

Instead of using different implementations of varying complexity for different TMOs, the proposed unified format allows utilizing the same implementation for all global TMOs. Only the values of 256 coefficients will be updated if a different TMO needs to be used. The tone-mapping process is simple and involves only a search in the 256×1 array to find the interval in which the HDR pixel value falls, followed by a linear transformation. This takes a tiny fraction of the time taken by the original tone-mapping algorithms, as shown in the design examples in the later sections and can be implemented in real time. The execution time depends solely on the size of the HDR image and is not affected by the choice of algorithm or type of image content. These characteristics can make the proposed format attractive for content producers, streaming services, and display manufacturers. In a typical scenario, the contents can be produced/streamed in the HDR format and tone-mapped in a short predictable time if the target display is LDR. The creative intent can be well-represented by the set of 256 coefficients, which can be embedded in the content.

To summarize the work, we present:

- A unified representation of global TMOs with only 256 floating-point numbers.
- An algorithm to obtain these coefficients for any global TMO.
- An efficient unified implementation of the global TMOs represented in the proposed compact format.
- Detailed experimental evaluation showing the accuracy of the proposed unified representation in replicating the original algorithms.
- Experimental results showing the time efficiency of the proposed implementation.

The rest of this paper is organized as follows. In Section 2, we explain the process of extracting 256 key points from a set of HDR and LDR images. Design examples and detailed experimental evaluations of the proposed representation of global TMOs are presented in Sections 3 and 4, respectively. A brief discussion on the results and some conclusions drawn from the work are described in Section 5.

2. Literature review

A plethora of tone-mapping techniques has been proposed over the past two decades. We describe a few representative ones here.

Some initial TMOs were based on a non-linear global transformation which enhanced the dark regions while compressing the brighter ones. A simple such algorithm would be to apply a log or gamma function to the HDR luminance. Drago et al. [8] adaptively changed the logarithmic base depending on the luminance value to achieve a better visual effect. Gamma correction is commonly used to map the contents on the screen in a traditional display. Qiao et al. [9] used a localized gamma correction in dark and bright regions to enhance contrast and adjust saturation. Reinhard et al. [5] performed local dodging and burning operations to brighten dark regions and push bright tones to darker levels, to give a photographic look to the tone-mapped images. While such transformations are very simple to apply, they usually do not produce the best results for all types of scenes.

Tone-mapping can be seen as a mechanism to distribute a few display levels among groups of pixels of similar intensities. Therefore, several TMOs are based on computing the histogram of the input HDR luminance and distributing the display levels among the histogram bins [3,10,11]. Histogram-based approaches can overstretch the contrast in more populated bins and overly compress it in the bins with very few pixels. Larson et al. [3] proposed a way to overcome this problem by clamping the pixel counts at a threshold and artificially increasing the counts of sparse bins to a defined minimum. Another measure taken by Khan et al. [4] was to non-uniformly construct the histogram bins following the sensitivity of the HVS in different brightness levels. Han et al. [12] included the effect of ambient light in their histogram-based approach, improving the contrast for outdoor image display. An advantage of histogram-based techniques is that they can be implemented using linear interpolation which is relatively simple operation. However, considering the large size of images, they still require processing on GPU or FPGA if the target is to process the images in real time.

Clustering-based techniques have also been used for tone-mapping, using the same idea of the distribution of display levels among the clusters. For clustering, in general, *k*-means or the Gaussian Mixture Model (GMM) clustering algorithm are utilized [13–15]. Clustering is, however, a slow process, and the resultant algorithms are generally inefficient.

Several models of HVS have been proposed in the literature and are often used in image enhancement applications. Since tone-mapping also focuses on beautifying the visual display of the image, HVS models are often utilized. Pattanaik et al. [16] developed a model for luminance, pattern, and color processing in the HVS to understand the effects of adaptation on spatial vision and used it for tone-mapping. Kuang et al. [17] proposed iCAM06 for tone-mapping, which models the spatial processing of the HVS for contrast enhancement, light adaptation for details enhancement in highlights and shadows, and color appearance prediction for better color reproduction. Some other works that used the HVS in their tone-mapping algorithm include [18,19]. All these techniques have very different algorithms and require different implementation structures, making it difficult to add a generic tone-mapping feature in the display devices.

Some task-specific designs have also been proposed. Jinno et al. [20] designed a TMO targeting the coding of HDR content in a two-layer format. While it achieves good compression, the visual quality of the images is not always high. One common distortion happens in the appearance of color after tone-mapping. Kim et al. [21] used a weighted least-square method to preserve the global contrast and applied a lightness correction step to reproduce the actual colors of the HDR scene. The additional steps however lead to increased algorithm complexity. Rahardja et al. [22] proposed an interactive TMO for large screens which tracks the user gaze and enhances the relevant regions for a better visual experience. This offers a practical solution for large size displays and works in real time, however customized hardware using an eye tracking device and GPU are needed for processing in a controlled environment. Deep neural networks have also been tried for tone-mapping [23]; however, they require very large amounts of training data to be able to perform well on a variety of HDR scenes.

3. A generic representation of global tone-mapping algorithms

In this section, we present a simple method to represent any global TMO accurately by an array of 256 coefficients. The complete flowchart of the proposed algorithm is shown in Figure 1 and explained in the following subsections. Throughout our writing, we make a distinction between the terms “tone-mapped value” and the “LDR value”. The former is referred to the floating-point number obtained right after transforming (tone-mapping) an HDR value, while the latter refers to the tone-mapped value after integer rounding in [0, 255] range.

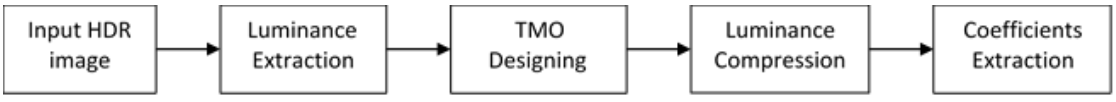

Figure 1. Structure of the proposed algorithm to represent any global TMO in a unified 256 × 1 format. The original TMO is used to tone-map the HDR luminance. From the HDR and tone-mapped luminance channels, 256 values are extracted that faithfully represent the original TMO. These steps are done in offline mode and coefficients are stored with the image.

3.1. Applying the original algorithm

The first step is to apply the original tone-mapping algorithm to the luminance channel of the HDR image. As shown in Figure 1, this operation comprises two modules—designing the tone-mapping scheme and compressing the luminance.

A global TMO typically begins with constructing the luminance channel from the red (R), green (G), and blue (B) channels of the HDR image by calculating their weighted average as:

$$Y_{HDR} = 0.265R + \ 0.670G + 0.065B. \tag{1}$$

Some TMOs use a different set of weights, but this does not affect the accuracy of our algorithm. The only requirement is to use the same weights here and in the modified algorithm presented later in this section.

The next step is to compress the luminance Y_{HDR} to obtain the tone-mapped luminance Y_T. Depending on the algorithm of the used TMO, this will require a different set of operations. We are only interested in the pair of HDR and tone-mapped luminance values, irrespective of the steps used to obtain them. Note that both HDR and tone-mapped values are in the floating-point format, i.e., rounding is not applied to the tone-mapped pixel values yet.

The last step in tone-mapping is to transform each color channel. We do not require this for the subsequent steps of our algorithm explained next, and therefore it is not mentioned in Figure 1.

3.2. Representation of TMO as an array of 256 coefficients

To represent the tone-mapping operation carried out by the original algorithm, we use an array of 256 coefficients. To generate this array, we consider the tone-mapped luminance Y_T obtained by the original TMO as a function of the original HDR luminance Y_{HDR}. This function is called the tone-mapping curve. We select some key points from the curve, such that the linear segments connecting them represent the curve accurately. These picked points are uniformly distributed between the minimum and maximum values of Y_T. The corresponding HDR values from Y_{HDR} are calculated through linear interpolation. For this, first, we construct a vector of 256 equispaced integer values as

$$\boldsymbol{l_m} = \{0, 1, 2, \ldots, 255\}. \tag{2}$$

These values are meant to serve as the key tone-mapped luminance values in the approximated tone-mapping curve. The idea here is that $\boldsymbol{l_m}$ can remain fixed for all TMOs and therefore does not need to be stored. The tone-mapped luminance is expected to be in the [0, 255] range, but many TMOs produce values beyond 255, which need to be clamped before display. To model the operation of all global TMOs, we assume that clamping is done at the final stage only after transforming the color channels. Therefore, we scale $\boldsymbol{l_m}$ to cover the full range of Y_T as follows:

$$\boldsymbol{l_{gm}} = \min(Y_T) + \frac{\boldsymbol{l_m}}{255}(\max(Y_T) - \min(Y_T)). \tag{3}$$

The next step is to find the HDR values corresponding to the vector $\boldsymbol{l_{gm}}$. This can be done through linear interpolation using the original tone-mapping curve, i.e., mutually mapping (Y_{HDR}, Y_T) pairs, obtained in Section 3.1 above. We denote this mapping as function *F* in the equation below:

$$\boldsymbol{h_{gm}} = \ F\left(\boldsymbol{l_{gm}}, Y_T, \ Y_{HDR}\right), \tag{4}$$

where $\boldsymbol{h_{gm}}$ denotes the HDR luminance values that would map to $\boldsymbol{l_{gm}}$. The function *F* works in two steps: it finds the interval in the LUT in which an input $\boldsymbol{l_{gm}}$ value falls and uses the two bounding

(Y_{HDR}, Y_T) pairs to perform linear interpolation. Denoting the bounding pairs as (Y_{H1}, Y_{T1}) and (Y_{H2}, Y_{T2}), an LDR value l from $\boldsymbol{l_{gm}}$ would map to the following HDR value:

$$h = Y_{H1} + \frac{(Y_{H2} - Y_{H1})(l - Y_{T1})}{(Y_{T2} - Y_{T1})}. \tag{5}$$

Here it should be noted that with the proposed uniform distribution of the LDR values in the LUT, the denominator term in (5) becomes a constant, which further simplifies the computation. Repeating (5) for all values in $\boldsymbol{l_{gm}}$, we obtain corresponding HDR values $\boldsymbol{h_{gm}}$. These $(\boldsymbol{h_{gm}}, \boldsymbol{l_{gm}})$ pairs are the set of points that can be connected using linear segments to represent the original tone-mapping curve. These pairs can be used to perform tone-mapping through linear interpolation and can produce results nearly identical to the output of the original TMO. It should be noted that only the minimum and maximum of the tone-mapped data Y_T are required to define $\boldsymbol{l_{gm}}$ in (3). These two values and the 256 floating-point values of $\boldsymbol{h_{gm}}$ are sufficient to define the whole tone-mapping algorithm.

Here it should be mentioned that some TMO designs are represented in the form of LUT comprising a few pairs of HDR and tone-mapped values. This LUT is used for tone-mapping the HDR image through linear interpolation. For such TMOs, we do not need to generate the tone-mapped luminance channel as discussed in Section 3.1. Instead, we can directly convert the LUT to the proposed 256x1 vector using the steps defined in (3), (4), and (5). The only difference will be that in (5), instead of Y_{HDR} and Y_T, the HDR and tone-mapped values in the LUT will be used respectively.

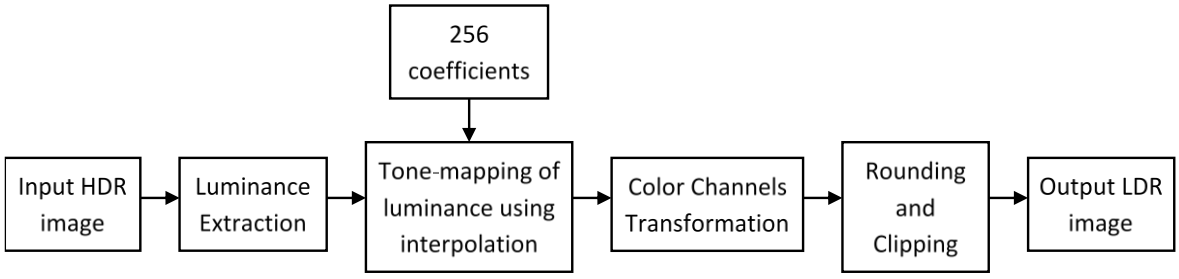

Figure 2. Flowchart of the tone-mapping steps using a TMO in the proposed format at the time of display. The luminance channel is tone-mapped first through interpolation using the 256 coefficients representing the TMO. This is followed by the transformation of the color channels.

3.3. Tone-mapping operation at the time of display

The above-mentioned operations of applying the original TMO to the luminance channel and extraction of 256 coefficients are carried out in the offline stage, and the extracted coefficients are stored with the image. At the time of display, these coefficients are used to replicate the original TMO

and generate LDR image. Figure 2 shows the steps involved in generating LDR image for display. First, the input HDR image is converted to the luminance channel using (1). Next, the dynamic range of the luminance channel of the HDR image is compressed. For this, the linear interpolation defined by (4) is used as:

$$Y_T' = F\left(Y_{HDR}, \boldsymbol{h_{gm}}, \boldsymbol{l_{gm}}\right). \tag{6}$$

Finally, the HDR and the tone-mapped luminance channels Y_{HDR} and Y_T' are used to compress the dynamic range of each color channel as:

$$(R,G,B)_T = \left(\frac{(R,G,B)_{HDR}}{Y_{HDR}}\right)^s \cdot Y_T', \tag{7}$$

where $s \leq 1$ is a saturation control user-defined parameter. Full saturation is achieved for $s = 1$, while the image will appear more desaturated for the smaller values. The output of (7) is in floating-point form, and therefore rounding is done when the image is displayed on an LDR screen or saved in an LDR image format. This can be expressed as:

$$(R,G,B)_{LDR} = |(R,G,B)_T|. \tag{8}$$

Any values above 255 are clamped for LDR display.

3.4. Complexity of real time tone-mapping operation

In the proposed method, tone-mapping can be implemented in real time in two steps, i.e., search in the array of 256 coefficients to determine the interval to which the input value belongs, followed by linear interpolation using endpoints of the found interval. The search has a complexity O(n *log*(k)) where n is the number of pixels and k is the number of elements in the array (i.e., 256). The linear interpolation step (3) requires only four summations and two multiplications. Therefore, the complexity of our implementation stays very low, at eight comparisons, two multiplications, and four additions, which is in O(n).

It should be that the proposed implementation can be used for any global tone-mapping algorithm. A different TMO will only require updating the 256 coefficients. These coefficients are used for linear interpolation to map the HDR luminance to LDR. Therefore, the design complexity depends only on the number of pixels in the image and stays the same for any global TMO represented using the proposed structure.

4. Experimental evaluations

4.1. Comparison of the tone-mapping curves

We present examples of three well-known global TMOs, Reinhard et al. [5], Kim and Kautz [7], and ATT [4], and show that our algorithm can represent them accurately as an array of 256 coefficients. In Figure 3, the top row shows the original and modified tone-mapping curves of each TMO for the test image "snow". It can be noted that the linear segments forming the modified curves provide very close approximations of the original curves. This indicates that the transformation from HDR to LDR using either the original or the modified curve will essentially produce nearly the same outputs. These

can be observed visually in Figure 3 from the tone-mapped versions of the test image produced by the original (shown in the middle row) and modified designs (shown in the bottom row) of each TMO.

4.2. Quantitative evaluations

We carried out some quantitative evaluations to further validate that the proposed unified 256x1 structure accurately represents the original TMOs. For these evaluations, we use the complete test dataset of 9 HDR images encoded in OpenEXR format on the accompanying DVD of [1] (courtesy Greg Ward). For comparison, the following full-reference image quality metrics are used: the peak signal-to-noise ratio (PSNR), the structural similarity (SSIM) index [24], the feature similarity (FSIM) index [25], the tone-mapped image quality index (TMQI) [26], and the feature similarity index for tone-mapped images (FSITM) [27].

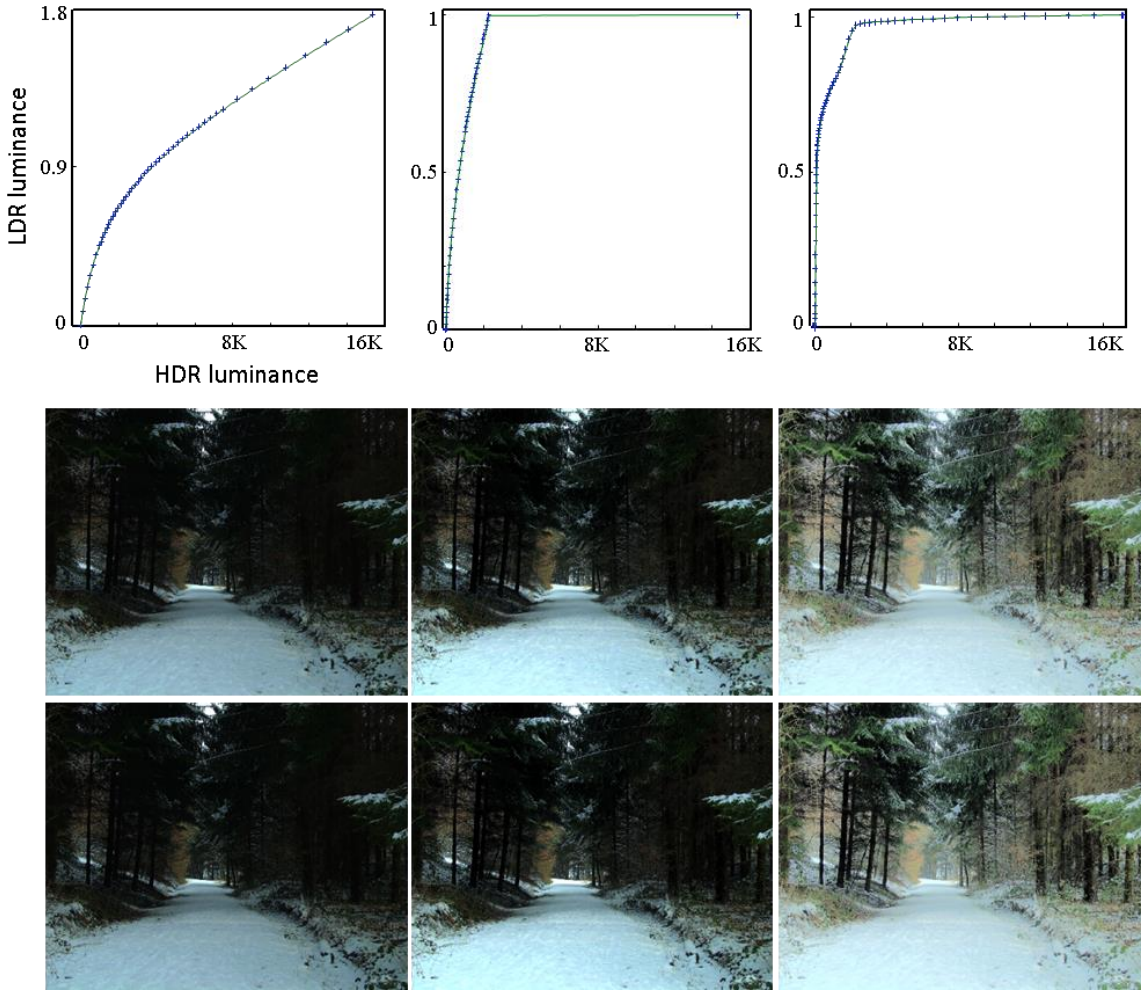

Figure 3. Comparison of original TMO designs with the proposed modified versions. The top row shows the original tone-mapping curves (solid lines) overlapped by the modified design curves (+ signs) of Reinhard's TMO (left), Kim's TMO (middle), and ATT (right) for test image "snow". The second and third rows show the tone-mapped results of the original and the modified designs, respectively. The curves of the original and modified designs overlap perfectly, and the output images are visually identical showing that the proposed algorithm precisely replicates the original algorithm.

PSNR and SSIM are well-known traditional metrics. FSIM index [25] is based on contrast-invariant phase congruency and contrast-dependent gradient magnitude. Both features play complementary roles and are combined into an overall quality score. FSIM, originally proposed for LDR images, was extended by Nafchi et al. [27] to FSITM which can be used to compare HDR and LDR images. FSITM focuses on how well the local angle maps are preserved and is calculated separately for each of the R, G, and B channels. TMQI [26] is the most popular among the existing methods to measure the quality of tone-mapped images. It is composed of two metrics – structure fidelity and statistical naturalness. Inspired by SSIM, structural fidelity compares the structure in reference and test image patches. If signal strengths of both HDR and LDR patches are above/below the visibility threshold, the structure is assumed to be intact. For naturalness, TMQI uses a blind approach utilizing the brightness and contrast attributes of the tone-mapped image. The ideal values of these attributes were determined by analyzing a large dataset of 3000 images of natural scenes.

The results of our experiments using these metrics are shown in Table 1. The PSNR, SSIM, and FSIM scores are calculated using the original algorithms' output images as the reference. The average scores shown in the table indicate a very high similarity in the output of the original TMOs and their proposed alternative representation. TMQI and FSITM metrics take the original HDR images as a reference and quantify the quality of the test images in [0, 1] range, where higher values indicate better quality. The average scores of both the original algorithms and their 256 × 1 representations are presented in Table 1, where the latter are shown in italic font. Both scores are nearly identical. These evaluations clearly show that the proposed 256 × 1 structure provides a very accurate alternate representation of the original algorithms and does not change their output.

Table 1. Accuracy of the proposed unified design in replicating the original TMOs using full-reference LDR and HDR metrics on a test dataset of 9 HDR images (courtesy Greg Ward). In the last two columns, scores of original methods are shown in plain font and those of modified versions in italic.

	PSNR	SSIM	FSIM	TMQI	FSITM
Modified and original ATT	73.765	1	1	0.9332	0.8831
				0.9331	*0.8832*
Modified and original Reinhard	54.948	0.9991	0.9998	0.7719	0.6246
				0.7717	*0.6247*
Modified and original Kim	45.253	0.9973	0.9973	0.8487	0.6555
				0.8491	*0.6558*

4.3. Subjective evaluations

We carried out a subjective study using the simultaneous double stimulus for continuous evaluation (SDSCE) method described in ITU-R BT.500-14 [28]. Fifteen non-expert observers of age in the range of [20, 25] years took part in this study and experimented using 20 HDR images picked randomly from the HDR dataset in RGBE format on the accompanying DVD of [36]. All participants had normal or corrected to normal visual acuity and normal color vision. They were shown pairs of reference (output of original TMO) and test (output of the proposed implementation) images one by one in a dim-light indoor environment on a 17-inch 1920 × 1080 HP monitor, placed on a desk approximately 40 cm away from the participant's chair. They were asked to score the similarity

between each pair in [0, 100] range, where a higher score means higher similarity, zero indicates clearly visible differences, and 100 refers to differences being completely imperceptible. The reference and test images were shown side by side on the monitor, and the participants were allowed to take as much time as needed to observe them. Using a 95% confidence interval [37], the mean value of the similarity scores stayed in the 94.9 ± 3.4 range. This high value strongly suggests that output images of the original and the modified algorithms are visually identical.

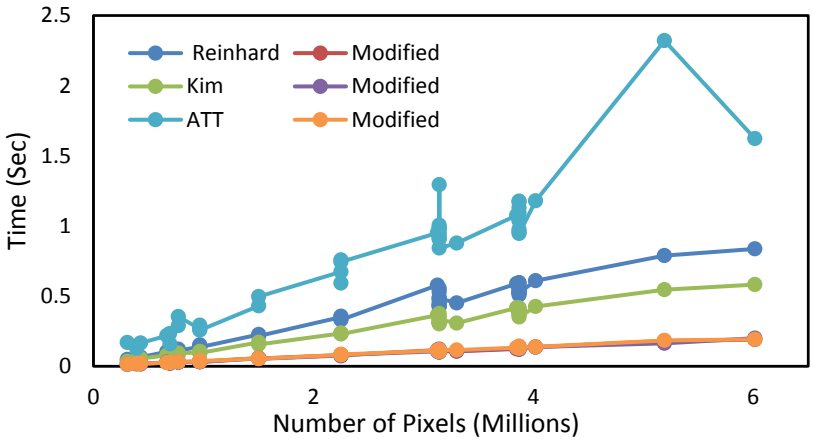

Figure 4. Execution times of the original algorithms and the proposed representations for a set of 42 HDR images.

4.4. Execution time

The evaluations reported above validate that the proposed unified representation of the global TMOs can accurately represent any global TMO. Next, we demonstrate the main benefit of the proposed unified structure, i.e., the reduction in tone-mapping time at the time of display.

We applied the original algorithms of three TMOs, Reinhard, Kim, and ATT, and their modified versions in the proposed format, to 42 different HDR images. The images had 13 unique resolutions, ranging from 3 Megapixels to 6 Megapixels. The top three curves in Figure 4 show the execution times of the original TMOs, whereas the three lines overlapping each other at the bottom show the execution times of the modified versions in the proposed format. Here, the following observations can be made:

1. The modified representation can run significantly faster. Even the largest image took less than 200 msec.
2. The three overlapping curves at the bottom representing the execution time of the proposed versions of the algorithms indicate that the execution time for each image of the same size remains the same. In other words, the execution time of the proposed implementation is independent of the original algorithm and depends solely on the number of pixels.
3. The execution times of the original algorithms do not necessarily increase linearly with image size. For example, in ATT, the step to determine the number of suitable histogram bins is an iterative process and takes unpredictable time. Therefore, even for images of the same size, the execution time can be different. In contrast, the execution time of our implementation is strictly the function of image size alone.

Here it should be mentioned that the proposed algorithm gains in execution speed from pre-calculation of the transformation coefficients during the offline stage. The contribution of the proposed algorithm is to represent any global TMO as a 256 × 1 array, thereby enabling an efficient unified implementation of all global TMOs using linear interpolation.

5. Conclusions

HDR images have potential applications wherever the quality of image can improve the analysis or visual experience. Some of these applications can be in virtual reality [29], gaming [30], scene analysis [31], license plate detection [32], and defect detection [33,34]. Advances in display technologies [35] are expected to increase the pace of adaptation of HDR content. However, the existing LDR displays require tone-mapping before the HDR content can be rendered on them. Tone-mapping techniques can retain the details of the HDR images in the tone-mapped LDR versions and many TMOs of different complexity levels exist in the literature.

Using piecewise linear segments, or LUTs, to represent the tone-mapping curves is not a new concept, and some existing TMOs based on the histogram are indeed implemented using LUTs and linear interpolation. Our proposed algorithm makes it possible to represent any global TMO in this form. In addition, we proposed to fix the LDR values of the LUT to an equally spaced set of 256 integer values. Therefore, the LUT is reduced to a 256 × 1 vector of floating-point HDR values only, and any global TMO can be represented in this unified structure and implemented through linear interpolation. We also presented an algorithm to extract these 256 coefficients automatically from a given pair of HDR and LDR images. It has been shown by design examples that the characteristics of the original design remain well preserved as the tone-mapped output images of the original and the proposed modified designs are almost identical. This allows us to represent all global TMOs with the same structure and realize them with the same implementation. Another significant consequence of this unified tone-mapping is that the execution time is dependent only on the image size irrespective of the original algorithm and therefore can be estimated beforehand. Moreover, the execution is very fast compared to the original algorithms. These characteristics increase the acceptability of the proposed structure for real time operations, in software as well as hardware. A limitation of the proposed algorithm however is that it works only for global TMOs. Local TMOs use many-to-many mappings and cannot be represented by a single vector.

The proposed unified representation of TMOs and their implementation can influence the way HDR contents are currently released, which are being produced in large quantities due to the availability of HDR cameras and displays. The proposed algorithm can advance the HDR research in multiple directions, and below we mention a few.

It is not always possible to implement a tone-mapping module with real time performance. Therefore, in the existing HDR content delivery systems, both HDR and LDR versions need to be produced to cater to different consumer needs. The proposed unified representation of TMOs with a small set of coefficients can enable usage of the same content for both HDR and LDR display. The coefficients that can represent the TMO can be extracted during the offline stage and released with the HDR content. Displaying this content on the HDR displays will be straightforward, while tone-mapping required before showing them on LDR displays can be carried out in real time at the time of display using our implementation. Emerging HDR formats such as HDR10 and Dolby Vision do not include this feature yet in their current releases.

The efficiency of operation, predictability of execution time, and a single unified implementation for all global TMOs are the features that can make the proposed unified structure and implementation desirable for a consumer electronics device such as a set-top box (STB) or TV. In a typical scenario, the contents produced in HDR format can be released along with the set of 256 coefficients, and a software/hardware module in the STB or the TV can tone-map them in real time for LDR display. If a different TMO needs to be used, it would require only updating the coefficients without changing the implementation structure. This can be an interesting feature for the display makers.

Since the TMO is represented just by 256 coefficients, which require negligible space compared to the image data, it is possible to embed multiple TMOs in the content. This would provide multiple options to generate content for LDR display as per user preference or depending on the viewing conditions. If a light sensor is available, as is case of smart phones, a suitable tone-mapping can be automatically picked for the best viewing experience depending on the environmental light.

Acknowledgments

This work was funded by the Deanship of Scientific Research (DSR), University of Jeddah, under grant No. UJ-28-18-DR. The authors, therefore, acknowledge with thanks DSR technical and financial support.

Conflict of interest

The authors have no conflict of interest.

References

1. E. Reinhard, G. Ward, S. Pattanaik, P. Debevec, *High Dynamic Range Imaging: Acquisition, Display and Image-Based Lighting, 2nd Edition*. Morgan Kaufmann, 2010.
2. X. Cerda-Company, C. A. Parraga, X. Otazu, Which tone-mapping operator is the best? A comparative study of perceptual quality, *J. Opt. Soc. Am.*, **35** (2018), 626–638. https://doi.org/10.1364/JOSAA.35.000626
3. G. W. Larson, H. Rushmeier, C. Piatko, A visibility matching tone reproduction operator for high dynamic range scenes, *IEEE Trans. Vis. Comput. Graph.*, **3** (1997), 291–306. https://doi.org/10.1109/2945.646233
4. I. R. Khan, S. Rahardja, M. M. Khan, M. M. Movania, F. Abed, A Tone-Mapping Technique Based on Histogram Using a Sensitivity Model of the Human Visual System, *IEEE Trans. Ind. Electron.*, **65** (2018), 3469–3479. https://doi.org/10.1109/TIE.2017.2760247
5. E. Reinhard, M. Stark, P. Shirley, J. Ferwerda, Photographic tone reproduction for digital images, *ACM Trans. Graph.*, **21** (2002), 267–276. https://doi.org/10.1145/566654.566575
6. J. De Praeter, A. J. Díaz-Honrubia, T. Paridaens, G. Van Wallendael, P. Lambert, Simultaneous encoder for high-dynamic-range and low-dynamic-range video, *IEEE Trans. Consum. Electron.*, **62** (2016), 420–428. https://doi.org/10.1109/TCE.2016.7838095
7. M. H. Kim, J. Kautz, Consistent tone reproduction, *Proc. Tenth IASTED Int. Conf. Comput. Graph. Imag.*, ACTA Press Anaheim, 2008, 152–159.
8. F. Drago, K. Myszkowski, T. Annen, N. Chiba, Adaptive Logarithmic Mapping for Displaying High Contrast Scenes, *Comput. Graph. Forum*, **22** (2003), 419–426. https://doi.org/10.1111/1467-8659.00689

9. M. Qiao, M. K. Ng, Tone mapping for high-dynamic-range images using localized gamma correction, *J. Electron. Imag.*, **24** (2015), 013010. https://doi.org/10.1117/1.JEI.24.1.013010
10. J. Duan, M. Bressan, C. Dance, G. Qiu, Tone-mapping high dynamic range images by novel histogram adjustment, *Pattern Recognit.*, **43** (2010), 1847–1862. https://doi.org/10.1016/j.patcog.2009.12.006
11. A. Boschetti, N. Adami, R. Leonardi, M. Okuda, High dynamic range image tone mapping based on local Histogram Equalization, *IEEE Int. Conf. Multimedia Expo (ICME)*, (2010), 1130–1135. https://doi.org/10.1109/ICME.2010.5583305
12. J. Han, I. R. Khan, S. Rahardja, Lighting condition adaptive tone mapping method, *ACM SIGGRAPH Posters*, (2018). https://doi.org/10.1145/3230744.3230773
13. H. Li, X. Jia, L. Zhang, Clustering based content and color adaptive tone mapping, *Comput. Vis. Image Underst.*, **168** (2018), 37–49. https://doi.org/10.1016/j.cviu.2017.11.001
14. W. U. Lee, S. Park, S. J. Ko, Image fusion-based tone mapping using gaussian mixture model clustering, *IEEE Int. Conf. Consum. Electron.*, (2020).
15. M. Oskarsson, Temporally Consistent Tone Mapping of Images and Video Using Optimal K-means Clustering, *J. Math. Imag. Vis.*, **57** (2017), 225–238. https://doi.org/10.1007/s10851-016-0677-1
16. S. N. Pattanaik, J. A. Ferwerda, M. D. Fairchild, D. P. Greenberg, A multiscale model of adaptation and spatial vision for realistic image display, *Conf. Comput. Graph. Interact. Tech. (SIGGRAPH)*, (1998), 287–298. https://doi.org/10.1145/280814.280922
17. J. Kuang, G. M. Johnson, M. D. Fairchild, iCAM06: A refined image appearance model for HDR image rendering, *J. Vis. Commun. Image Represent.*, **18** (2007), 406–414. https://doi.org/10.1016/j.jvcir.2007.06.003
18. N. H. Nguyen, T. Van Vo, Y. Jeong, Y. Moon, C. Lee, Optimized Tone Mapping of HDR Images via HVS Model-Based 2D Histogram Equalization, *APSIPA Trans. Signal Inf. Process.*, (2018), 700–704. https://doi.org/10.23919/APSIPA.2018.8659452
19. I. R. Khan, W. Aziz, S. O. Shim, Tone-Mapping Using Perceptual-Quantizer and Image Histogram, *IEEE Access*, **8** (2020), 31350–31358. https://doi.org/10.1109/ACCESS.2020.2973273
20. T. Jinno, M. Okuda, N. Adami, New local tone mapping and two-layer coding for HDR images, *IEEE Int. Conf. Acoust. Speech Signal Process., (ICASSP)*, (2012), 765–768. https://doi.org/10.1109/ICASSP.2012.6287996
21. B. K. Kim, R. H. Park, S. K. Chang, Tone mapping with contrast preservation and lightness correction in high dynamic range imaging, *Signal Image Video Process.*, **10** (2016), 1425–1432. https://doi.org/10.1007/s11760-016-0942-1
22. S. Rahardja, F. Farbiz, C. Manders, Z. Huang, J. Ling, I. Khan, et al., Eye hdr: Gaze-adaptive system for displaying high-dynamic-range images, *SIGGRAPH ASIA Art Gallery & Emerging Technologies: Adaptation*, (2009), 68. https://doi.org/10.1145/1665137.1665187
23. C. Guo, X. Jiang, Deep Tone-Mapping Operator Using Image Quality Assessment Inspired Semi-Supervised Learning, *IEEE Access*, **9** (2021), 73873–73889. https://doi.org/10.1109/ACCESS.2021.3080331
24. Z. Wang, A. C. Bovik, H. R. Sheikh, E. P. Simoncelli, Image quality assessment: from error visibility to structural similarity, *IEEE Trans. Image Process.*, **13** (2004), 600–612. https://doi.org/10.1109/TIP.2003.819861
25. L. Zhang, L. Zhang, X. Mou, D. Zhang, FSIM: A feature similarity index for image quality assessment, *IEEE Trans. Image Process.*, **20** (2011), 2378–2386.

https://doi.org/10.1109/TIP.2011.2109730
26. H. Yeganeh, Z. Wang, Objective quality assessment of tone-mapped images, *IEEE Trans. Image Process.*, **22** (2013), 657–667. https://doi.org/10.1109/TIP.2012.2221725
27. Z. H. Nafchi, A. Shahkolaei, R. Farrahi Moghaddam, M. Cheriet, FSITM: A Feature Similarity Index For Tone-Mapped Images, *IEEE Signal Process. Lett.*, **22** (2015), 1026–1029. https://doi.org/10.1109/LSP.2014.2381458
28. BT.500: Methodologies for the subjective assessment of the quality of television images, available from: https://www.itu.int/rec/R-REC-BT.500 (accessed Feb. 18, 2022).
29. G. Somanath, D. Kurz, HDR Environment Map Estimation for Real-Time Augmented Reality, *IEEE/CVF Conf. Comput. Vision Pattern Recognit. (CVPR)*, (2021), 11298–11306. https://doi.org/10.1109/CVPR46437.2021.01114
30. A. Khaldieh, S. Ploumis, M. T. Pourazad, P. Nasiopoulos, V. Leung, Tone mapping for video gaming applications, 2018 *IEEE Int. Conf. Consumer Electron. (ICCE)*, (2018), 1–12. https://doi.org/10.1109/ICCE.2018.8326304
31. M. Purohit, M. Singh, A. Kumar, B. K. Kaushik, Enhancing the Surveillance Detection Range of Image Sensors Using HDR Techniques, *IEEE Sensors J.*, **21** (2021), 19516–19528. https://doi.org/10.1109/JSEN.2021.3091018
32. S. T. A. Ali, A. H. Usama, I. R. Khan, M. M. Khan, A. Siddiq, Mobile registration number plate recognition using artificail intelligence, *2021 IEEE Int. Conf. Image Process. (ICIP)*, (2021), 944–948. https://doi.org/10.1109/ICIP42928.2021.9506699
33. J. Ahmed, B. Gao, W. L. Woo, Sparse Low-Rank Tensor Decomposition for Metal Defect Detection Using Thermographic Imaging Diagnostics, *IEEE Trans. Ind. Inform.*, **17** (2021), 1810–1820. https://doi.org/10.1109/TII.2020.2994227
34. B. Hu, B. Gao, W. L. Woo, L. Ruan, J. Jin, Y. Yang, et al., A Lightweight Spatial and Temporal Multi-Feature Fusion Network for Defect Detection, *IEEE Trans. Image Process.*, **30** (2021), 472–486. https://doi.org/10.1109/TIP.2020.3036770
35. S. S. Kaderuppan, E. W. L. Wong, A. Sharma, W. L. Woo, Smart Nanoscopy: A Review of Computational Approaches to Achieve Super-Resolved Optical Microscopy, *IEEE Access*, **8** (2020), 214801–214831. https://doi.org/10.1109/ACCESS.2020.3040319

AIMS Press